JAERI-M
86-086

NEANDC (J) 121/U
INDC (JPN) 107/L

EVALUATION OF NEUTRON NUCLEAR DATA FOR ^{250}Cf and ^{251}Cf

June 1986

Tsuneo NAKAGAWA

日本原子力研究所
Japan Atomic Energy Research Institute

JAERI-Mレポートは，日本原子力研究所が不定期に公刊している研究報告書です。
入手の問合わせは，日本原子力研究所技術情報部情報資料課（〒319-11茨城県那珂郡東海村）あて，お申しこしください。なお，このほかに財団法人原子力弘済会資料センター（〒319-11 茨城県那珂郡東海村日本原子力研究所内）で複写による実費頒布をおこなっております。

JAERI-M reports are issued irregularly.
Inquiries about availability of the reports should be addressed to Information Division Department of Technical Information, Japan Atomic Energy Research Institute, Tokai-mura, Naka-gun, Ibaraki-ken 319-11, Japan.

編集兼発行　日本原子力研究所
印　　刷　いばらき印刷㈱

JAERI-M 86-086

Evaluation of Neutron Nuclear Data for ^{250}Cf and ^{251}Cf

Tsuneo NAKAGAWA

Department of Physics

Tokai Research Establishment
Japan Atomic Energy Research Institute
Tokai-mura, Naka-gun, Ibaraki-ken

(Received May 21,1986)

Nuclear data of ^{250}Cf and ^{251}Cf have been evaluated in the energy range from 10^{-5} eV to 20 MeV. There exist only a few experimental data for the cross sections of both the isotopes, that is, the cross sections at the thermal neutron energy and the resonance integrals. Therefore, the present evaluation was based on systematic trends of the data and the calculation with the optical, statistical and evaporation models. Cross sections evaluated in this work are the total, elastic and inelastic scattering, fission, radiative capture, (n,2n), (n,3n) and (n,4n) reaction cross sections. In the energy range below 150 eV, hypothetical resonance levels were generated so as to reproduce the measured thermal cross sections and resonance integrals. Other evaluated quantities are the angular distributions of elastically and inelastically scattered neutrons and those of neutrons emitted from the (n,2n), (n,3n), (n,4n) and fission reactions, their energy distributions, and average numbers of neutrons emitted per fission. The results were compiled in the ENDF/B-V format.

This work was performed under contracts between Power Reactor and Nuclear Fuel Development Corporation and Japan Atomic Energy Research Institute.

Keywords: Californium-250, Californium-251, Evaluation, Cross Section, Angular Distribution, Energy Distribution, Optical Model, Statistical Model, Evaporation Model

JAERI－M 86－086

^{250}Cfと^{251}Cfの中性子核データの評価

日本原子力研究所東海研究所物理部
中川　庸雄

（1986年5月21日受理）

^{250}Cfと^{251}Cfの核データ評価を，10^{-5} eVから20 MeVまでの中性子エネルギー範囲で行った。両核種とも，断面積の測定値は少なく，わずかに，熱中性子エネルギーでの断面積，および共鳴積分値の測定があるだけである。従って今回の評価は，主としてデータの系統性と光学模型，統計模型および蒸発模型による理論計算を利用して行った。評価した断面積は，全断面積，弾性および非弾性散乱断面積，核分裂断面積，中性子捕獲断面積，(n,2n)，(n,3n) および (n,4n) 反応断面積である。150 eV以下では，熱中性子エネルギー断面積と共鳴積分の測定値を再現するような仮想共鳴レベルを発生させた。この他，弾性散乱，非弾性散乱および(n, 2n)，(n, 3n)，(n, 4n)，核分裂反応後の放出中性子の角分布，エネルギー分布，そして核分裂当りの平均放出中性子数の評価を行った。結果はENDF/B－Vフォーマットで編集した。

東海研究所：〒319－11　茨城県那珂郡東海村白方字白根2－4
本報告書は，日本原子力研究所が動力炉・核燃料開発事業団の委託により行った研究の成果である。

Contents

目　　次

1. Introduction

Precise Knowledge of nuclear data for transplutonium isotopes is important for analysis of the higher actinide productions in the nuclear fuel cycle. We performed, therefore, the evaluation work on the neutron nuclear data of ^{241}Am, ^{242g}Am, ^{242m}Am, ^{243}Am, ^{242}Cm, ^{243}Cm, ^{244}Cm and ^{245}Cm, and stored them in JENDL-2. After compilation of JENDL-2, the nuclear data of ^{246}Cm, ^{247}Cm, ^{248}Cm, ^{249}Cm, ^{249}Bk and ^{249}Cf have been evaluated for JENDL-3. In the fiscal year of 1985, the data of ^{250}Cf and ^{251}Cf were evaluated under contracts with Power Reactor and Nuclear Fuel Development Corporation.

These two nuclides are on the ^{252}Cf production path, and have the α-decay half-lives of 13.08 years and 898 years, respectively. Experiments on their neutron data have not been performed so many times. Only their thermal data are available at present. Consequently, the present evaluation was mainly based on systematics from data of neighboring nuclides. Table 1 is a list of the quantities evaluated in the present work.

2. Data in Resonance Region

2.1 Thermal Cross Sections

(a) Californium-250

Measured values of the thermal cross sections are shown in Table 2. The radiative capture cross sections are largely scattered from 1090 to 2034 barns. The recent two measurements by Halperin et al.[5] and Gavrilov and Goncharov[6] are in good agreement with each other. In the present evaluation, the cross section of 1730 ± 220 barns was adopted by averaging the measured values of Folger et al.[3] and of the recent two experiments.

1. Introduction

Precise Knowledge of nuclear data for transplutonium isotopes is important for analysis of the higher actinide productions in the nuclear fuel cycle. We performed, therefore, the evaluation work on the neutron nuclear data of ^{241}Am, ^{242g}Am, ^{242m}Am, ^{243}Am, ^{242}Cm, ^{243}Cm, ^{244}Cm and ^{245}Cm, and stored them in JENDL-2. After compilation of JENDL-2, the nuclear data of ^{246}Cm, ^{247}Cm, ^{248}Cm, ^{249}Cm, ^{249}Bk and ^{249}Cf have been evaluated for JENDL-3. In the fiscal year of 1985, the data of ^{250}Cf and ^{251}Cf were evaluated under contracts with Power Reactor and Nuclear Fuel Development Corporation.

These two nuclides are on the ^{252}Cf production path, and have the α-decay half-lives of 13.08 years and 898 years, respectively. Experiments on their neutron data have not been performed so many times. Only their thermal data are available at present. Consequently, the present evaluation was mainly based on systematics from data of neighboring nuclides. Table 1 is a list of the quantities evaluated in the present work.

2. Data in Resonance Region

2.1 Thermal Cross Sections

(a) Californium-250

Measured values of the thermal cross sections are shown in Table 2. The radiative capture cross sections are largely scattered from 1090 to 2034 barns. The recent two measurements by Halperin et al.[5] and Gavrilov and Goncharov[6] are in good agreement with each other. In the present evaluation, the cross section of 1730 ± 220 barns was adopted by averaging the measured values of Folger et al.[3] and of the recent two experiments.

The measurement of the fission cross section was made by Metta et al.[2] However, they could not find any evidence of the thermal neutron induced fission. The value compiled in EXFOR is 'less than 350 barns'. In the present evaluation, the small fission cross section of about a few barns was assumed.

(b) Californium 251

Table 3 lists the values of measured thermal cross sections of ^{251}Cf. The radiative capture cross section was measured by Mugnusson et al.[1] and by Halperin et al.[5] Since both results are in good agreement with each other, the experimental value of Halperin et al., 2850 ± 150 barns, was adopted in the present evaluation.

The four measurements of the fission cross section were reported so far. Recent results are larger than older ones. We assumed the fission cross section of 4890 ± 190 barns that was obtained by averaging the recent experimental values measured by Ragaini et al.[7] and Flynn et al.[8] Consequently, sum of the radiative capture and fission cross sections of 7740 barns became larger than measured absorption cross sections. It seems that there exists inconsistency among experimental data.

2.2 Resonance Integrals

The resonance integral of the ^{250}Cf radiative capture cross section was measured by Halperin et al.[5], and by Gavrilov and Goncharov[6], and that of the absorption cross section was obtained by Folger et al.[3] Large discrepancies are found among measured values as shown in Table 4. The value of 8300 ± 3300 barns was adopted in the present evaluation by averaging the two recent measurements. The resonance integral of 1600

barns was adopted for the ^{251}Cf radiative capture cross section on the basis of the measurement by Halperin et al.[5)]

No experimental data are available on the fission resonance integrals of both the isotopes.

2.3 Resonance Parameters

2.3.1 Resolved Resonance Parameters

No experimental data of the resonance parameters are existing for both the nuclides. Hence, hypothetical resonance levels were generated with almost the same method as that proposed by McCrosson[9)] so as to reproduce the thermal cross sections and resonance integrals mentioned above. For the generation of resonance levels and their parameters, average radiative capture and fission widths, neutron strength functions, level spacings and effective scattering radii must be reasonably assumed. In the present evaluation, they were determined as follows:

(a) Radiative capture width

Theoretical prediction of radiative capture widths for the transactininum isotopes was made by Moore.[10)] We adopted his results;

Γ_γ = 36.9 meV for ^{250}Cf,

Γ_γ = 43.5 meV for ^{251}Cf.

(b) Fission width

The average fission width was estimated from the thermal cross sections and radiative capture width as follows.

$$\Gamma_f = \frac{\sigma_f}{\sigma_\gamma} \times \Gamma_\gamma . \qquad (1)$$

The fission width of 74.6 meV was obtained for ^{251}Cf by adopting σ_f = 4890 barns, σ_γ = 2850 barns and Γ_γ = 43.5 meV. In the case of ^{250}Cf, the fission width of 0.1 meV was assumed because no thermal cross section has been measured and a very small value could be expected.

(c) Neutron strength functions

The optical model calculation described in Chapter 3 predicts the s-wave strength function of 0.831×10^{-4} for both isotopes in the low neutron energy region. This values seems to be slightly smaller than S_0 values of other neighboring nuclides.[11] Hence, in this work, the s-wave neutron strength function of 1.0×10^{-4} was adopted for both isotopes.

(d) Average level spacing

The average level spacing for s-wave resonances was calculated from a level density formula. Level density parameters were derived from resonance level spacings of the neighboring nuclides[11] and level schemes as described in Chapter 3. The calculated s-wave level spacings are 16 eV and 6.3 eV for ^{250}Cf and ^{251}Cf, respectively.

(e) Effective scattering radii

The effective scattering radii were estimated from the optical model calculation; R = 9.253 fm for ^{250}Cf and R = 9.252 for ^{251}Cf.

By using these basic parameters, hypothetical s-wave levels were generated below 190 eV including a negative energy level. The energies and parameters of the negative and the first positive levels were adjusted so as to reproduce the thermal cross sections and resonance

integrals. The single-level Breit-Wigner formula was used to calculate the resonance cross sections. The upper boundary of the resolved resonance region was set at 150 eV.

2.3.2 Unresolved Resonance Parameters

In the energy range from 150 eV to 30 keV, unresolved resonance parameters were evaluated for both isotopes. Those of ^{250}Cf were based on the average parameters used in the resolved resonance region, and the p-wave strength function of 3.0×10^{-4} obtained with the optical model calculation.

As for ^{251}Cf, the average resonance parameters adopted in the resolved resonance region gave too small fission cross sections at higher energies. Hence, the average fission with and neutron strength functions were adjusted so as to reproduce the reasonable values of the fission cross section.

The effective scattering radii were adjusted to the total cross section calculated at 30 keV. These obtained unresolved resonance parameters are summarized in Table 5.

3. Cross Sections above Resonance Region

3.1 Fission Cross Section

No measurements have been made for the fission cross section in the fast neutron energy region. Therefore, the cross section was determined from systematics. Behrens and Howerton[12] obtained an empirical formula for the fission cross sections relative to that of ^{235}U in the energy range from 3 to 5 MeV. Recently, Lasijo[13] tried to find an alternative empirical formula on the basis of the same experimental data as those used by Behrens and Howerton. He found the following formula.

integrals. The single-level Breit-Wigner formula was used to calculate the resonance cross sections. The upper boundary of the resolved resonance region was set at 150 eV.

2.3.2 Unresolved Resonance Parameters

In the energy range from 150 eV to 30 keV, unresolved resonance parameters were evaluated for both isotopes. Those of ^{250}Cf were based on the average parameters used in the resolved resonance region, and the p-wave strength function of 3.0×10^{-4} obtained with the optical model calculation.

As for ^{251}Cf, the average resonance parameters adopted in the resolved resonance region gave too small fission cross sections at higher energies. Hence, the average fission with and neutron strength functions were adjusted so as to reproduce the reasonable values of the fission cross section.

The effective scattering radii were adjusted to the total cross section calculated at 30 keV. These obtained unresolved resonance parameters are summarized in Table 5.

3. Cross Sections above Resonance Region

3.1 Fission Cross Section

No measurements have been made for the fission cross section in the fast neutron energy region. Therefore, the cross section was determined from systematics. Behrens and Howerton[12] obtained an empirical formula for the fission cross sections relative to that of ^{235}U in the energy range from 3 to 5 MeV. Recently, Lasijo[13] tried to find an alternative empirical formula on the basis of the same experimental data as those used by Behrens and Howerton. He found the following formula.

$$\sigma_f = F(Z) + C \times [N-G(Z)]^2, \quad (2)$$

where Z is the atomic number and N the neutron number, and F(Z) and G(Z) are given as

$$G(Z) = a_0 + a_1 Z + a_2 Z^2, \quad (3)$$

$$a_0 = -2690.37063,$$

$$a_1 = 59.7373309,$$

$$a_2 = -0.3138082,$$

$$F(Z) = b_0 + b_1 Z + b_2 Z^2 + b_3 Z^3, \quad (4)$$

$$b_0 = 2815.607814,$$

$$b_1 = -89.65620409,$$

$$b_2 = 0.94850607,$$

$$b_3 = -0.00333247,$$

and the constant C is 0.01702407. Figures 1 and 2 show the fission cross sections for various nuclides predicted from Eq. 2 together with the experimental data. The fission cross sections of ^{250}Cf and ^{251}Cf are estimated to be 2.323 and 2.406 barns, respectively.

Shape of the fission cross section in the high energy region was determined from systematic trends of adjacent nuclides. In the low energy region, they were represented with the resolved and unresolved resonance parameters. The two parts of cross section were connected smoothly by eye-guiding in the medium energy region.

3.2 (n,2n), (n,3n) and (n,4n) Reaction Cross Sections

These cross sections were calculated with Pearlstein's method[14]. The neutron emission cross section is nearly equal to the difference between the compound nucleus formation cross section calculated with the optical model and the fission cross section, because the charged particle emission cross sections are negligibly small. A part of the

neutron emission cross section, about 10 mb, was assumed to be the inelastic scattering cross section in the high energy region.

The Q-values of the (n,2n), (n,3n) and (n,4n) reactions were obtained from the compilation of mass excess by Wapstra and Bos[15], and are given in Table 6. The ^{250}Cf (n,4n) reaction was ignored in the present calculation because its threshold energy is very high.

3.3 Level Density Parameters

Level density parameters were newly determined on the basis of Gilbert-Cameron's composite formula[16]. For determination of the parameters, the computer program LEVDENS[17] was used.

Pairing energies and shell corrections were taken as they were given by Gilbert and Cameron. The spin cutoff factor was assumed to be

$$\sigma_M^2 = 0.146\sqrt{aU}A^{2/3} = \alpha_M\sqrt{U}. \qquad (5)$$

The parameter a was determined so that the measured s-wave level spacings recommended by Mughabghab[11] might be obtained well. Figure 3 shows the obtained a parameters. The a parameters of ^{250}Cf and ^{251}Cf were estimated from systematic trend shown in Fig. 3.

The number of low energy levels is expressed with the constant temperature model as

$$N(E) = C\times T\exp(E/T). \qquad (6)$$

The constant C and nuclear temperature T were determined from staircase plots of low-lying levels[21,22]. An example of ^{250}Cf is given in Fig. 4. The obtained level density parameters of Cf isotopes are listed in Table 7. In the table, the parameters Δ and E_x are the pairing energy and the connecting energy of the constant temperature model and the Fermi gas model.

3.4 Other Cross Sections

Other cross sections were calculated with the program CASTHY[18] based on the spherical optical and statistical models. The optical potential parameters shown in Table 8 were obtained by Igarasi and Nakagawa[19] so as to reproduce the total cross section of ^{241}Am measured by Phillips and Howe.[20]

Taking the (n,2n), (n,3n), (n,4n) and fission as the competing processes, the radiative capture, elastic and inelastic scattering cross sections were calculated. The same average radiative capture widths and s-wave level spacings as those in the resonance region were used for calculation of the capture cross sections.

$\langle\Gamma_\gamma\rangle$ = 0.0369 eV, D_0 = 16 eV, for ^{250}Cf,

$\langle\Gamma_\gamma\rangle$ = 0.0435 eV, D_0 = 6.3 eV, for ^{251}Cf.

The data on discrete levels were taken from the Nuclear Data Sheets[21,22]. The adopted levels are given in Tables 9 and 10, for ^{250}Cf and ^{251}Cf, respectively. The twenty-nine excited levels up to 1.478 MeV were taken into account for ^{250}Cf and levels above 1.50 MeV were assumed to be overlapping. The 500-keV level with $J^\pi = 8^+$ was ignored because of small contribution to the cross section. On the other hand, the twenty-three levels up to 649 keV were adopted for ^{251}Cf, and levels above 700 keV were assumed to be overlapping. Although several levels have very large spin values, all of them were taken into the present calculation.

4. Other Quantities

4.1 Angular Distributions of Emitted Neutrons

The angular distributions of elastically and inelastically scattered neutrons were calculated with the optical and statistical

3.4 Other Cross Sections

Other cross sections were calculated with the program CASTHY[18] based on the spherical optical and statistical models. The optical potential parameters shown in Table 8 were obtained by Igarasi and Nakagawa[19] so as to reproduce the total cross section of ^{241}Am measured by Phillips and Howe.[20]

Taking the (n,2n), (n,3n), (n,4n) and fission as the competing processes, the radiative capture, elastic and inelastic scattering cross sections were calculated. The same average radiative capture widths and s-wave level spacings as those in the resonance region were used for calculation of the capture cross sections.

$\langle\Gamma_\gamma\rangle$ = 0.0369 eV, D_0 = 16 eV, for ^{250}Cf,

$\langle\Gamma_\gamma\rangle$ = 0.0435 eV, D_0 = 6.3 eV, for ^{251}Cf.

The data on discrete levels were taken from the Nuclear Data Sheets[21,22]. The adopted levels are given in Tables 9 and 10, for ^{250}Cf and ^{251}Cf, respectively. The twenty-nine excited levels up to 1.478 MeV were taken into account for ^{250}Cf and levels above 1.50 MeV were assumed to be overlapping. The 500-keV level with $J^\pi = 8^+$ was ignored because of small contribution to the cross section. On the other hand, the twenty-three levels up to 649 keV were adopted for ^{251}Cf, and levels above 700 keV were assumed to be overlapping. Although several levels have very large spin values, all of them were taken into the present calculation.

4. Other Quantities

4.1 Angular Distributions of Emitted Neutrons

The angular distributions of elastically and inelastically scattered neutrons were calculated with the optical and statistical

models. The isotropic distributions in the laboratory system were assumed for the neutrons emitted from the continuum inelastic scattering, fission, (n,2n), (n,3n) and (n,4n) reactions.

4.2 Energy Distributions of Emitted Neutrons

Energy distributions of emitted neutrons were estimated with the same method as our previous evaluations. The evaporation spectrum was assumed for neutrons due to the continuum inelastic scattering. The nuclear temperature θ was determined as

$$\theta = T, \qquad \text{for } E_{n=}\leq E_x, \qquad (7)$$

$$\theta = \{1 + \sqrt{1+4a(E_n-\Delta)}\}/2a, \qquad \text{for } E_n > E_x. \qquad (8)$$

where E_n is the incident neutron energy, and a and Δ are the level density parameter and the pairing energy of the residual nucleus. The parameter T is the nuclear temperature defined in the constant temperature model (Eq. 6), and E_x is the energy where the constant temperature model is connected to the Fermi gas model.

The neutron spectra from the (n,2n), (n,3n) and (n,4n) reactions were also characterized with the evaporation model. The Maxwellian spectrum was adopted for the fission neutrons. The temperature was estimated from the systematics obtained by Smith et al.[23)]

4.3 Average Numbers of Neutrons Emitted per Fission

(a) Prompt neutrons

Howerton[24,25)] obtained the following semi-empirical formula on the average number of neutrons emitted per neutron-induced fission for the target nucleus with the mass number of A and the atomic number of Z.

$$\bar{\nu}(Z,A,E_n) = 2.33+0.06[2-(-1)^{A+1-Z}-(-1)^{Z}]+0.15(Z-92)+0.02(A-235) +[0.130+0.006(A-235)]\times[E_n-E_{th}(Z,A)] \qquad (9)$$

where E_n is the incident neutron energy. The fission threshold energy E_{th} is written as

$$E_{th}(Z,A) = 18.6-0.36Z^2/(A+1)+0.2[2-(-1)^{A+1-Z}-(-1)^Z]-B_n, \quad (10)$$

where B_n stands for the neutron separation energy from compound nucleus. This formula predicts the number of neutrons as

$$\bar{\nu}_p = 3.63+0.220E_n, \quad \text{for } ^{250}\text{Cf}, \quad (11)$$

$$\bar{\nu}_p = 3.84+0.226E_n, \quad \text{for } ^{251}\text{Cf}. \quad (12)$$

Equation 11 was adopted for ^{250}Cf. As for ^{251}Cf, the number of prompt neutrons was measured by Flynn et al.[8] for the thermal-neutron-induced fission; $\bar{\nu}_p = 4.1 \pm 0.5$. Therefore, we adopted the expression.

$$\bar{\nu}_p = 4.1+0.226E_n, \quad \text{for } ^{251}\text{Cf}. \quad (12')$$

(b) Delayed neutrons

The following systematics on the number of delayed neutrons was proposed by Tuttle[26]:

$$\bar{\nu}_d = \exp[13.81+0.1754(A_c-3Z)(A_c/Z)], \quad (13)$$

where A_c is the mass number of the compound nucleus. We assumed that since the (n,n'f) channel opens around 7 MeV, the (n,n'f) process is always dominant above 7 MeV. The values of $\bar{\nu}_d$ at lower energies and at higher energies were linearly connected between 6 and 8 MeV.

^{250}Cf $\quad \bar{\nu}_d$=0.00406 (E_n<6 MeV),
0.00280 (E_n>8 MeV).

^{251}Cf $\quad \bar{\nu}_d$=0.00590 (E_n<6 MeV),
0.00406 (E_n>8 MeV).

5. Comparison with Other Evaluations

The evaluated nuclear data of ^{250}Cf and ^{251}Cf are existing in the

where E_n is the incident neutron energy. The fission threshold energy E_{th} is written as

$$E_{th}(Z,A) = 18.6-0.36Z^2/(A+1)+0.2[2-(-1)^{A+1-Z}-(-1)^Z]-B_n, \quad (10)$$

where B_n stands for the neutron separation energy from compound nucleus. This formula predicts the number of neutrons as

$$\bar{\nu}_p = 3.63+0.220E_n, \quad \text{for } ^{250}\text{Cf}, \quad (11)$$

$$\bar{\nu}_p = 3.84+0.226E_n, \quad \text{for } ^{251}\text{Cf}. \quad (12)$$

Equation 11 was adopted for ^{250}Cf. As for ^{251}Cf, the number of prompt neutrons was measured by Flynn et al.[8] for the thermal-neutron-induced fission; $\bar{\nu}_p = 4.1 \pm 0.5$. Therefore, we adopted the expression.

$$\bar{\nu}_p = 4.1+0.226E_n, \quad \text{for } ^{251}\text{Cf}. \quad (12')$$

(b) Delayed neutrons

The following systematics on the number of delayed neutrons was proposed by Tuttle[26]:

$$\bar{\nu}_d = \exp[13.81+0.1754(A_c-3Z)(A_c/Z)], \quad (13)$$

where A_c is the mass number of the compound nucleus. We assumed that since the (n,n'f) channel opens around 7 MeV, the (n,n'f) process is always dominant above 7 MeV. The values of $\bar{\nu}_d$ at lower energies and at higher energies were linearly connected between 6 and 8 MeV.

^{250}Cf $\quad \bar{\nu}_d$=0.00406 (E_n<6 MeV),

0.00280 (E_n>8 MeV).

^{251}Cf $\quad \bar{\nu}_d$=0.00590 (E_n<6 MeV),

0.00406 (E_n>8 MeV).

5. Comparison with Other Evaluations

The evaluated nuclear data of ^{250}Cf and ^{251}Cf are existing in the

ENDF/B-V[27] and ENDL[28] also. The evaluation for the ENDL is essentially the same as that of the ENDF/B-V. The present results are, therefore, compared with the ENDF/B-V in Figs. 5 to 14.

Figures from 5 to 9 show the data of ^{250}Cf. Cross sections in the resolved resonance region are averaged in suitable energy intervals in the figures. Hypothetical resonance levels were also generated in the ENDF/B-V evaluation so as to reproduce the thermal cross sections and resonance integrals. Since the level generation was based on the same way as the present evaluation, the both results show the same trend in general. However, the large discrepancies exist in the elastic scattering and fission cross sections. The discrepancies come from the different treatments of the negative resonance as to the elastic scattering cross section. The present evaluation introduced the negative resonance, while the ENDF/B-V evaluation gave background cross sections in place of the negative resonance. The fission cross sections displayed in Fig. 7 also have large discrepancy below 1 MeV. The ENDF/B-V adopted the cross section of 0.0 barn at the thermal energy. Figure 9 shows comparison of the inelastic scattering, (n,2n) and (n,3n) cross sections. In the energy region below a few hundred keV, the present result of the inelastic scattering is larger than the ENDF/B-V. In the other region, the present results of the threshold reactions are smaller. This seems to be caused by the difference of the fission cross sections.

Figures from 10 to 14 compare the data of ^{251}Cf. The same tendency as ^{250}Cf is found in the resonance cross sections, except the fission cross section which is in better agreement than ^{250}Cf. The reason is that there exist the measured fission cross sections at the thermal neutron energy. The trend of the threshold reactions is the same as ^{250}Cf.

Table 11 lists the thermal cross sections and resonance integrals calculated from the present evaluation and the ENDF/B-V. Both results are in very good agreement with experimental data.

6. Concluding Remarks

The neutron nuclear data of ^{250}Cf and ^{251}Cf have been evaluated in the energy range from 10^{-5} eV to 20 MeV. All cross sections obtained are shown in Figs. 15 and 16. By taking account of systematics of data and theoretical calculations, reasonable evaluated data were obtained. Large discrepancies are existing between present results and ENDF/B-V evaluation. These discrepancies are due to lack of experimental data.

The available experimental cross section data are only the thermal cross sections and resonance integrals. As shown in Chapter 2, scattering of the experimental data is large. Measurements of resonance parameters in the low energy region and the fission cross section in the high energy region are required in order to perform more accurate evaluation.

Acknowledgment

The author thanks members of the Nuclear Data Center of JAERI for their helpful discussion. He also appreciates Dr. Lasijo who tried to make the alternative systematics of the fission cross section, and Dr. Iijima (NAIG) for his advice on level density parameters.

References

1) Magnusson, L.B., Studier, M.H., Fields, P.R., Stevens, C.M., Mech, J.F., Friedman, A.M., Diamond, H. and Huizenga, J.R.: Phys. Rev., 96, 1576 (1976).

Table 11 lists the thermal cross sections and resonance integrals calculated from the present evaluation and the ENDF/B-V. Both results are in very good agreement with experimental data.

6. Concluding Remarks

The neutron nuclear data of ^{250}Cf and ^{251}Cf have been evaluated in the energy range from 10^{-5} eV to 20 MeV. All cross sections obtained are shown in Figs. 15 and 16. By taking account of systematics of data and theoretical calculations, reasonable evaluated data were obtained. Large discrepancies are existing between present results and ENDF/B-V evaluation. These discrepancies are due to lack of experimental data.

The available experimental cross section data are only the thermal cross sections and resonance integrals. As shown in Chapter 2, scattering of the experimental data is large. Measurements of resonance parameters in the low energy region and the fission cross section in the high energy region are required in order to perform more accurate evaluation.

Acknowledgment

The author thanks members of the Nuclear Data Center of JAERI for their helpful discussion. He also appreciates Dr. Lasijo who tried to make the alternative systematics of the fission cross section, and Dr. Iijima (NAIG) for his advice on level density parameters.

References

1) Magnusson, L.B., Studier, M.H., Fields, P.R., Stevens, C.M., Mech, J.F., Friedman, A.M., Diamond, H. and Huizenga, J.R.: Phys. Rev., 96, 1576 (1976).

Table 11 lists the thermal cross sections and resonance integrals calculated from the present evaluation and the ENDF/B-V. Both results are in very good agreement with experimental data.

6. Concluding Remarks

The neutron nuclear data of ^{250}Cf and ^{251}Cf have been evaluated in the energy range from 10^{-5} eV to 20 MeV. All cross sections obtained are shown in Figs. 15 and 16. By taking account of systematics of data and theoretical calculations, reasonable evaluated data were obtained. Large discrepancies are existing between present results and ENDF/B-V evaluation. These discrepancies are due to lack of experimental data.

The available experimental cross section data are only the thermal cross sections and resonance integrals. As shown in Chapter 2, scattering of the experimental data is large. Measurements of resonance parameters in the low energy region and the fission cross section in the high energy region are required in order to perform more accurate evaluation.

Acknowledgment

The author thanks members of the Nuclear Data Center of JAERI for their helpful discussion. He also appreciates Dr. Lasijo who tried to make the alternative systematics of the fission cross section, and Dr. Iijima (NAIG) for his advice on level density parameters.

References

1) Magnusson, L.B., Studier, M.H., Fields, P.R., Stevens, C.M., Mech, J.F., Friedman, A.M., Diamond, H. and Huizenga, J.R.: Phys. Rev., 96, 1576 (1976).

Table 11 lists the thermal cross sections and resonance integrals calculated from the present evaluation and the ENDF/B-V. Both results are in very good agreement with experimental data.

6. Concluding Remarks

The neutron nuclear data of ^{250}Cf and ^{251}Cf have been evaluated in the energy range from 10^{-5} eV to 20 MeV. All cross sections obtained are shown in Figs. 15 and 16. By taking account of systematics of data and theoretical calculations, reasonable evaluated data were obtained. Large discrepancies are existing between present results and ENDF/B-V evaluation. These discrepancies are due to lack of experimental data.

The available experimental cross section data are only the thermal cross sections and resonance integrals. As shown in Chapter 2, scattering of the experimental data is large. Measurements of resonance parameters in the low energy region and the fission cross section in the high energy region are required in order to perform more accurate evaluation.

Acknowledgment

The author thanks members of the Nuclear Data Center of JAERI for their helpful discussion. He also appreciates Dr. Lasijo who tried to make the alternative systematics of the fission cross section, and Dr. Iijima (NAIG) for his advice on level density parameters.

References

1) Magnusson, L.B., Studier, M.H., Fields, P.R., Stevens, C.M., Mech, J.F., Friedman, A.M., Diamond, H. and Huizenga, J.R.: Phys. Rev., 96, 1576 (1976).

2) Metta, D., Diamond, H., Barnes, R.F., Milsted, J., Gray, Jr., J., Henderson, D.J. and Stevens, C.M.: J. Inorg. Nucl. Chem., 27, 33 (1965).

3) Folger, R.L., Smith, J.A., Brown, L.C., Overman, R.F. and Holcomb, H.P.: Proc. of Conf. on Nucl. Cross Sections and Technol., Washington D.C., 4-7 March 1968, NBS special publication 299, 1279 (1968).

4) Smith, J.A., Banick, C.J., Folger, R.L., Holcomb, H.P. and Richter, I.B.: Proc. of Conf. on Nucl. Cross Sections and Technol., Washington D.C., 4-7 March 1968, NBS special publication 299, 1285 (1968).

5) Halperin, J., Bermis, Jr., C.E., Druschel, R.E. and Eby, R.E.: "The Thermal Cross Sections and Resonance Integrals for Neutron Capture of ^{249}Cf, ^{250}Cf and ^{251}Cf", ORNL-4706, 47 (1971).

6) Gavrilov, V.D. and Goncharov, V.A.: Sov. At. Energy, 44, 274 (1978).

7) Ragaini, R.C., Hulet, E.K., Louheed, R.W. and Wild, J.: Phys. Rev., C9, 399 (1974).

8) Flynn, K.F., Gindler, J.E., Sjoblom, R.K. and Glendenin, L.E.: Phys. Rev., C11, 1676 (1975).

9) McCrosson, F.J.: Proc. of Conf. on Neutron Cross Sections and Technol., Knoxville, 15-17 March 1971, 714 (1971).

10) Moore, M.S.: Proc. of International Conf. on Neutron Phys. and Nucl. Data for Reactors and Other Applied Purposes, Harwell, 25-29 September 1978, 313 (1978).

11) Mughabghab, S.F.: "Neutron Cross Sections, Vol. 1, Neutron Resonance Parameters and Thermal Cross Sections, Part B, Z=61-100", Academic Press (1984).

12) Behrens, J.W. and Howerton, R.J.: Nucl. Sci. Eng., 65, 464 (1978).

13) Lasijo, R.S.: private communication (1986).

14) Pearlstein, S.: Nucl. Sci. Eng., 23, 238 (1965).

15) Wapstra, A.H. and Bos, K.: Atomic Data and Nucl. Data Tables, 19, No. 3 (1977).

16) Gilbert, A. and Cameron, A.G.W.: Can. J. Phys., 43, 1446 (1965).

17) Iijima, S.: private communication (1985).

18) Igarasi, S.: J. Nucl. Sci. Technol., 12, 67 (1975).

19) Igarasi, S. and Nakagawa, T.: "Evaluation of Neutron Nuclear Data for ^{242}Cm", JAERI-M 8342 (1979) [in Japanese].

20) Phillips, T.W. and Howe, R.E.: Nucl. Sci. Eng., 69, 375 (1979).

21) Schmorak, M.R.: Nucl. Data Sheets, 32, 87 (1981).

22) Schmorak, M.R.: Nucl. Data Sheets, 34, 1 (1981).

23) Smith, A., Guenther, P., Winkler, G. and McKnight, R.: "Prompt-Fission-Neutron Spectra of ^{233}U, ^{235}U, ^{239}Pu and ^{240}Pu relative to that of ^{252}Cf", ANL/NDM-50 (1979).

24) Howerton, R.J.: Nucl. Sci. Eng., 46, 42 (1971).

25) Howerton, R.J.: Nucl. Sci. Eng., 62, 438 (1977).

26) Tuttle, R.J.: Proc. of Consaltants' Meeting on Delayed Neutron Properties, Vienna, 26-30 March 1979, INDC(NDS)-107/G+Special, 29 (1979)

27) ENDF/B-V data file for ^{250}Cf (MAT=8850) and ^{251}Cf (MAT=8851), BNL-NCS-17541 (ENDF-201), 3rd Edition (ENDF/B-V), edited by Kinsey, R. (1979).

28) Howerton, R.J., Dye, R.E. and Perkins, S.T.: "The Neutron Library (ENDL82) in the Transmittal Format", UCRL-50400, Vol. 4, Rev. 1, Appendix C (1982).

Table 1 Quantities evaluated in the present work

Quantities	Energy range	
	^{250}Cf	^{251}Cf
1) Resonance parameters		
Resolved resonances	-1.58 - 177.0 eV	-0.35 - 189.8 eV
Resolved resonance region	10^{-5} - 150 eV	10^{-5} - 150 eV
Unresolved resonance region	0.15 - 30.0 keV	0.15 - 30.0 keV
2) Cross sections		
Total	10^{-5} eV - 20 MeV	10^{-5} eV - 20 MeV
Elastic scattering	10^{-5} eV - 20 MeV	10^{-5} eV - 20 MeV
Inelastic scattering	42.89keV- 20 MeV	24.92keV- 20 MeV
Fission	10^{-5} eV - 20 MeV	10^{-5} eV - 20 MeV
Radiative capture	10^{-5} eV - 20 MeV	10^{-5} eV - 20 MeV
(n,2n)	6.650 - 20 MeV	5.132 - 20 MeV
(n,3n)	12.27 - 20 MeV	11.78 - 20 MeV
(n,4n)	not given	17.40 - 20 MeV
3) Angular distributions of emitted neutrons		
Angular distributions of elastically and inelastically scattered neutrons, and those from (n,2n), (n,3n), (n,4n) and fission reactions were given in the same energy range as their cross-section data.		
4) Energy distributions of emitted neutrons		
Inelastic to continuum levels	1.506 - 20 MeV	0.703 - 20 MeV
Fission	10^{-5} eV - 20 MeV	10^{-5} eV - 20 MeV
(n,2n)	6.650 - 20 MeV	5.132 - 20 MeV
(n,3n)	12.27 - 20 MeV	11.78 - 20 MeV
(n,4n)	not given	17.40 - 20 MeV
5) Other quantities		
$\bar{\nu}_d$	10^{-5} eV - 20 MeV	10^{-5} eV - 20 MeV
$\bar{\nu}_p$	10^{-5} eV - 20 MeV	10^{-5} eV - 20 MeV
$\bar{\nu}_{tot}$	10^{-5} eV - 20 MeV	10^{-5} eV - 20 MeV

Table 2 Thermal cross sections of ^{250}Cf

(barns)

Authors	capture	fission
Mugnusson et al.[1]	∿ 1500	
Metta et al.[2]		< 350**
Folger et al.[3]	1500*	
Smith et al.[4]	1090*	
Halperin et al.[5]	2034 ± 200	
Gavrilov and Goncharov[6]	1800	
adopted	1730 ± 220	a few barns

* absorption cross sections

** from EXFOR 12562

Table 3 Thermal cross sections of ^{251}Cf

(barns)

Authors	capture	fission	absorption
Mugnusson et al.[1]	∿ 3000		
Metta et al.[2]		3000 ± 260	
Folger et al.[3]			6600
Smith et al.[4]		3500	4970
Halperin et al.[5]	2850 ± 150		
Ragaini et al.[7]		4800 ± 250	
Flynn et al.[8]		5300 ± 530	
adopted	2850 ± 150	4890 ± 190	7740

Table 4 Resonance integrals of radiative capture cross sections

(barns)

Authors	^{250}Cf	^{251}Cf
Folger et al.[3]	5300*	900*
Halperin et al.[5]	11600 ± 500	1600 ± 30
Gavrilov and Goncharov[6]	5000	
adopted	8300 ± 3300	1600 ± 30

* absorption cross section, and cutoff energy of 0.92 eV

Table 5 Unresolved resonance parameters

Quantity	^{250}Cf	^{251}Cf
energy range	150 eV ∿ 30 keV	150 eV ∿ 30 keV
scattering radius	9.112 fm	8.842 fm
level spacing	16 eV	6.3 eV
S_0	1.0×10^{-4}	0.843×10^{-4}
S_1	3.0×10^{-4}	4.56×10^{-4}
$\langle\Gamma_\gamma\rangle$	36.9 meV	43.5 meV
$\langle\Gamma_f\rangle$	0.1 meV	281 meV (ℓ=0)
		551 meV (ℓ=1)

Table 6 Q-values and threshold energies of (n,Xn) reactions

Reaction	Q-value(MeV)	E_{th}(MeV)
a) Californium-250		
(n,2n)	-6.6235	6.6502
(n,3n)	-12.2166	12.2659
(n,4n)*	-19.1953	19.2722
b) Californium-251		
(n,2n)	-5.1115	5.1320
(n,3n)	-11.7350	11.7821
(n,4n)	-17.3281	17.3977

*) the (n,4n) reaction of ^{250}Cf was ignored in the present evaluation.

Table 7 Level density parameters of Californium isotopes

Parameter	^{248}Cf	^{249}Cf	^{250}Cf	^{251}Cf	^{252}Cf
a(MeV^{-1})	29.4	29.9	31.2	32.2	31.6
α_M($MeV^{-1/2}$)	31.25	31.60	32.36	32.97	32.74
Δ(MeV)	1.16	0.77	1.673	0.77	1.635
T(MeV)	0.3693	0.3693	0.4025	0.3809	0.3927
C(MeV^{-1})	1.625	5.416	2.093	14.84	1.895
E_x(MeV)	3.954	3.636	5.418	4.204	5.233

Table 8 Optical potential parameters

(MeV and fm)

$V_0 = 43.4 - 0.107\ E_n$

$W_s = 6.95 - 0.339\ E_n + 0.0531\ E_n^2$

$V_{so} = 7.0$

$r_0 = r_{so} = 1.282$

$r_s = 1.29$

$a = a_{so} = 0.60$

$b = 0.50$

Potential V(r) is given as

$$V(r) = -V_0 f_1(r) - iW_s f_2(r) - V_{so}\left(\frac{h}{m_\pi c}\right)^2 \left|\frac{df_3(r)}{dr}\right| \frac{1}{r}(\vec{\sigma}\cdot\vec{\ell}),$$

where

$$f_1(r) = 1/[1 + \exp(\frac{r-R_0}{a})],$$

$$f_2(r) = 4\exp(\frac{r-R_s}{b})/[1+\exp(\frac{r-R_s}{b})],$$

$$f_3(r) = 1/[1 + \exp(\frac{r-R_{so}}{a_{so}})],$$

$$R_0 = r_0 A^{1/3},$$

$$R_s = r_s A^{1/3},$$

$$R_{so} = r_{so} A^{1/3}.$$

Table 9 Level scheme of ^{250}Cf

No.	Energy (keV)	Spin and parity	No.	Energy (keV)	Spin and parity
ground	0.0	0 +	15	1209.98	2 -
1	42.722	2 +	16	1211.	3 -
2	141.886	4 +	17	1244.51	2 +
3	296.25	6 +	18	1255.47	4 -
4	871.64	2 -	19	1266.65	0 +
5	905.90	3 -	20	1296.64	2 +
6	952.07	4 -	21	1311.07	5 -
7	1008.6	5 -	22	1335.	3 -
8	1031.85	2 +	23	1377.83	6 -
9	1070.	6 -	24	1385.49	(1 +)
10	1071.38	3 +	25	1396.16	5 -
11	1123.	4 +	26	1411.34	(1 +)
12	1154.23	0 +	27	1426.86	3 -
13	1175.52	1 -	28	1457.83	6 -
14	1189.40	2 +	29	1478.45	5 -

The 500-keV(8+) was ignored in the present calculation. Levels above 1.5 MeV were assumed to be overlapping.

Table 10 Level scheme of ^{251}Cf

No.	Energy (keV)	Spin and parity	No.	Energy (keV)	Spin and parity
ground	0.0	1/2 +	12	295.7	13/2 +
1	24.825	3/2 +	13	319.29	9/2 +
2	47.828	5/2 +	14	325.35	13/2 +
3	105.73	7/2 +	15	370.39	11/2 -
4	106.304	7/2 +	16	392.0	11/2 +
5	146.46	9/2 +	17	424.10	15/2 +
6	166.31	9/2 +	18	434.3	9/2 -
7	177.69	3/2 +	19	442.	13/2 -
8	211.72	5/2 +	20	514.	11/2 -
9	237.76	11/2 +	21	544.05	5/2 +
10	239.34	11/2 +	22	590.18	7/2 +
11	258.44	7/2 +	23	649.2	9/2 +

Levels above 700 keV were assumed to be overlapping.

Table 11 Comparison of thermal cross sections and resonance integrals

(barns)

	2200-m/s values		Resonance integrals*	
	capture	fission	capture	fission
1) Californium-250				
Present	1779	4.09	8420	27.8
ENDF/B-V	1611	0.0	11200	0.012
Experiment	1730±220	∿ 0	8300±3300	
2) Californium-251				
Present	2878	4935	1610	2780
ENDF/B-V	2862	5321	1630	4960
Experiment	2850±150	4890±190	1600±30	

* cutoff energy of 0.5 eV.

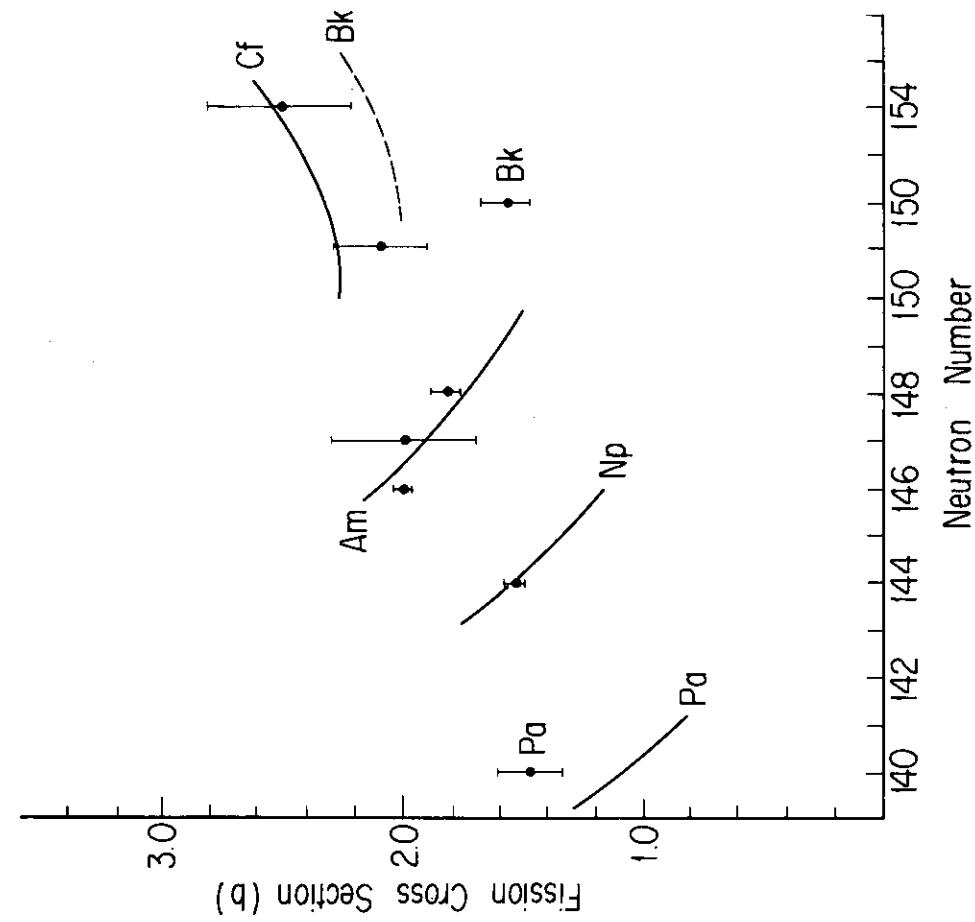

Fig. 1 Systematics of the fission cross section (1)

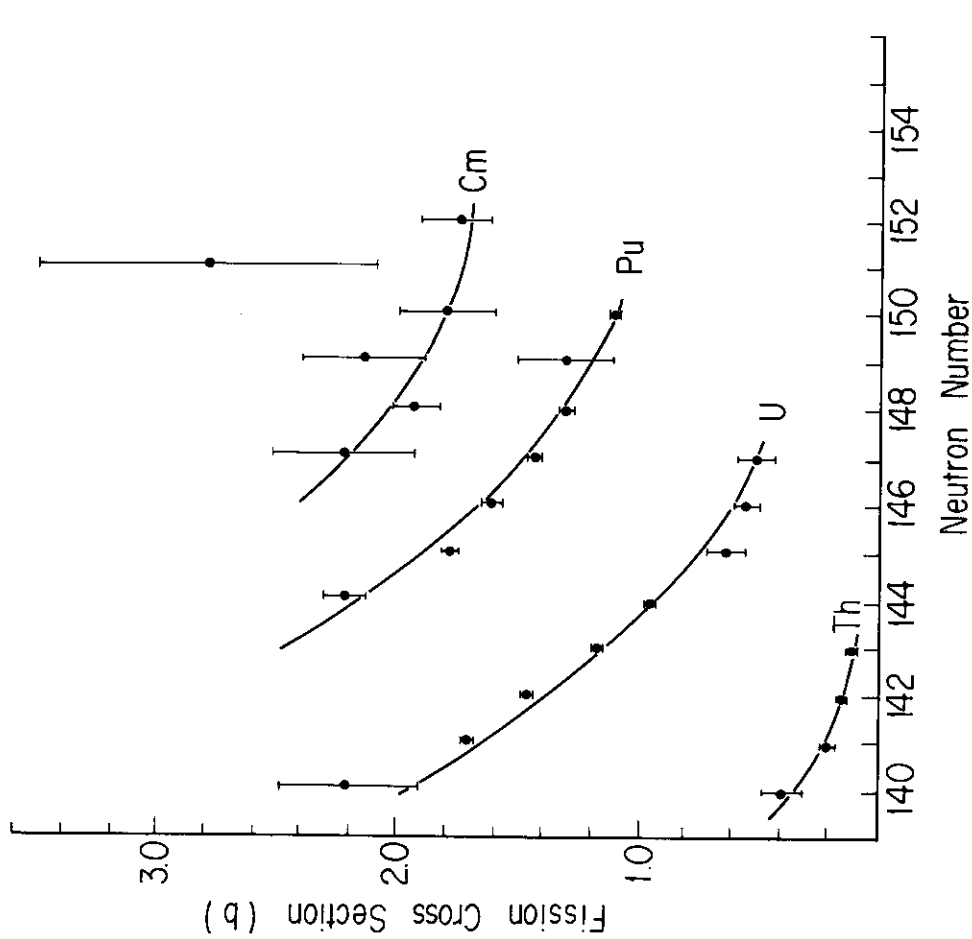

Fig. 2 Systematics of the fission cross section (2)

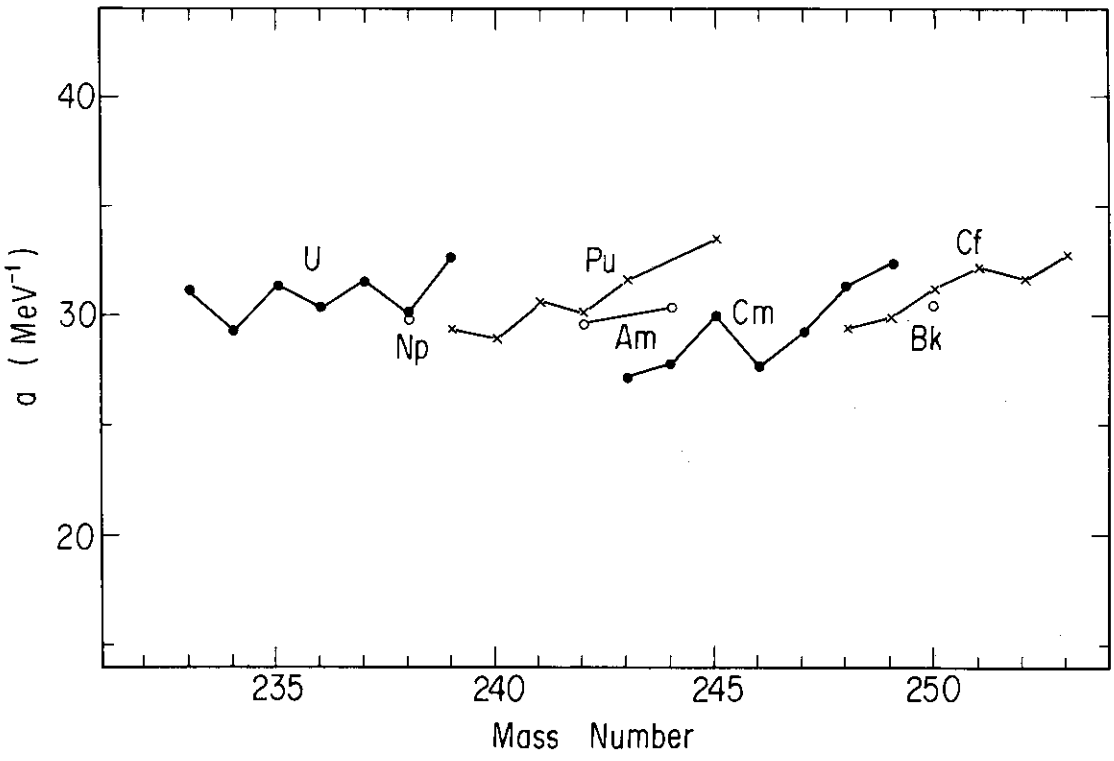

Fig. 3 a parameters of transactinium isotopes

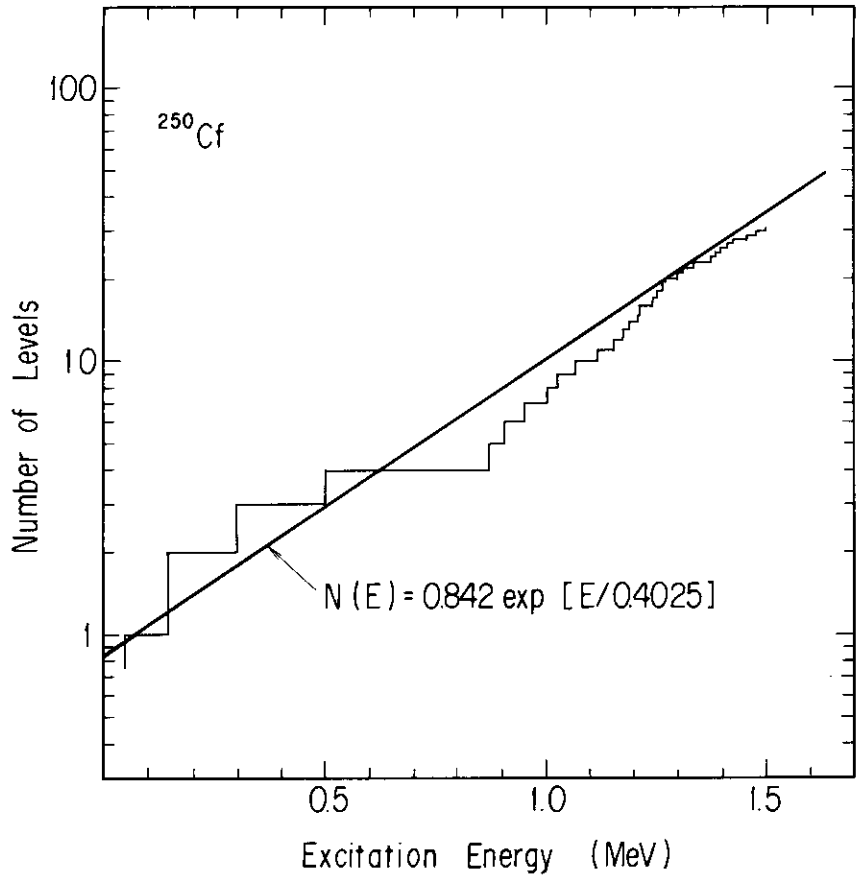

Fig. 4 Determination of level density parameters

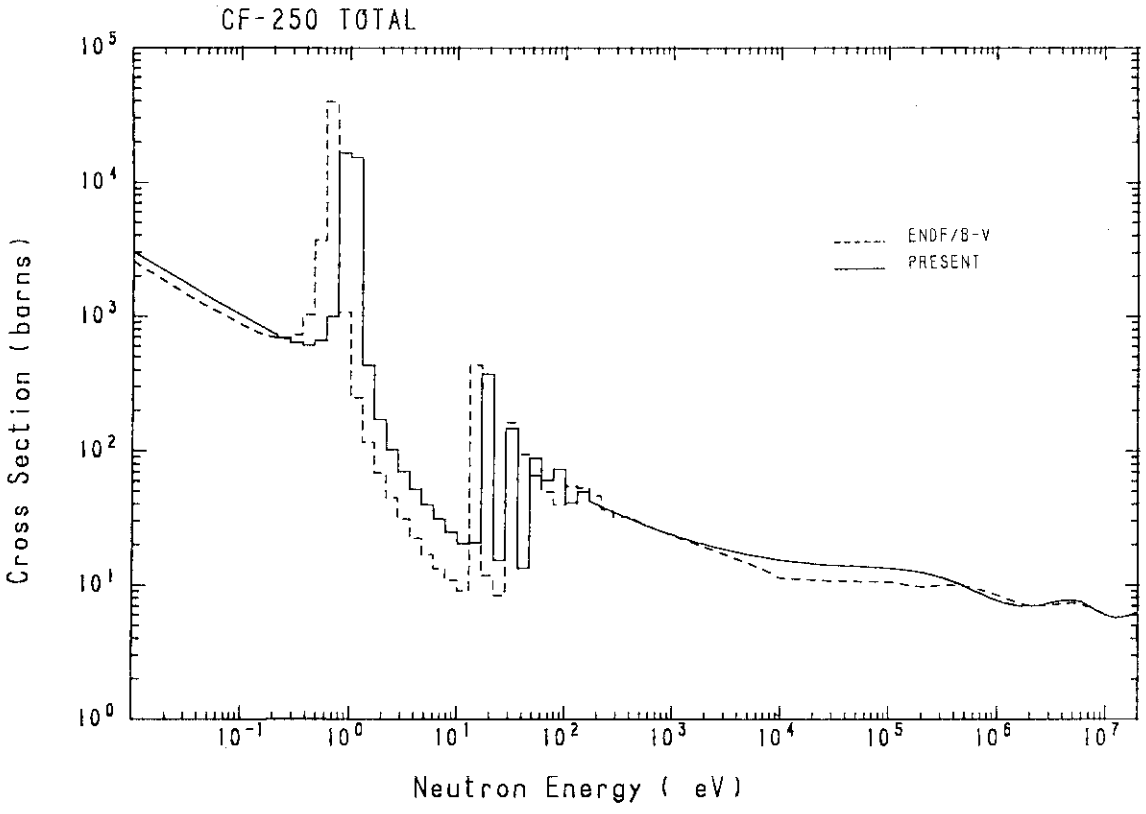

Fig. 5 The total cross section of ^{250}Cf
Cross sections in the resolved resonance region are averaged in suitable energy intervals.

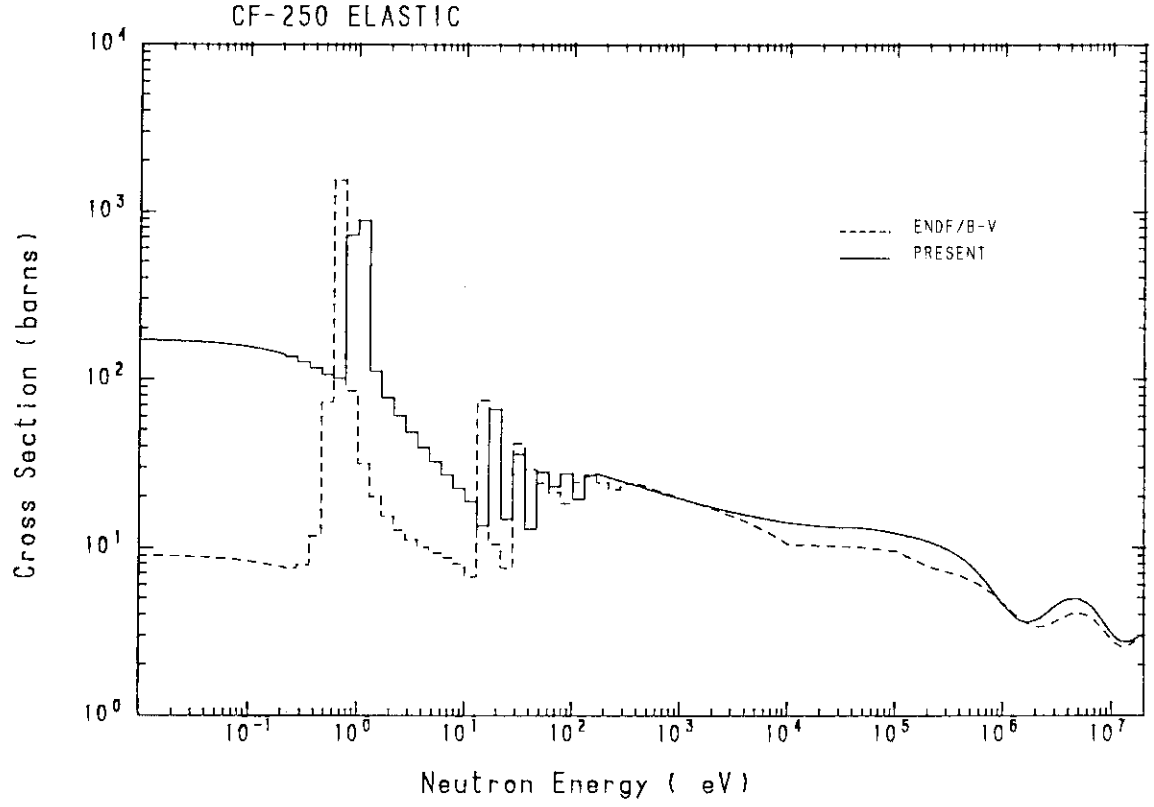

Fig. 6 The elastic scattering cross section of ^{250}Cf

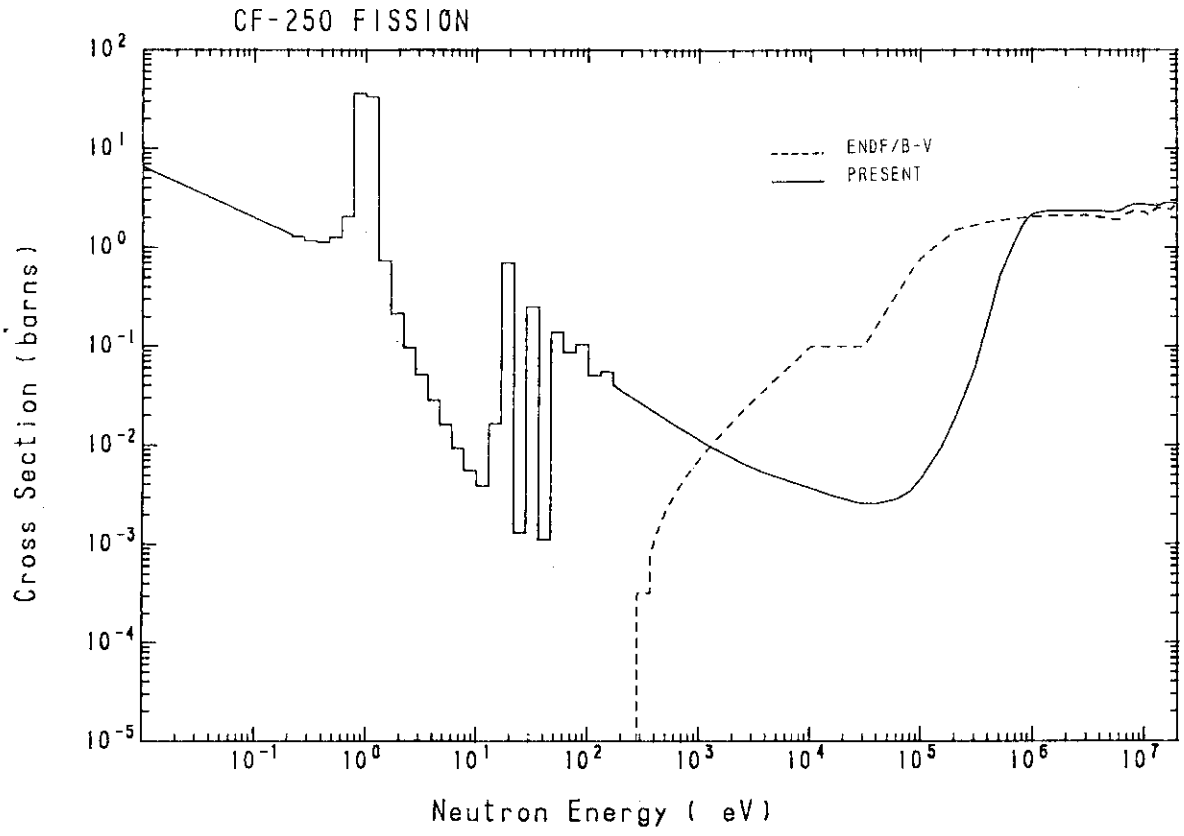

Fig. 7 The fission cross section of ^{250}Cf

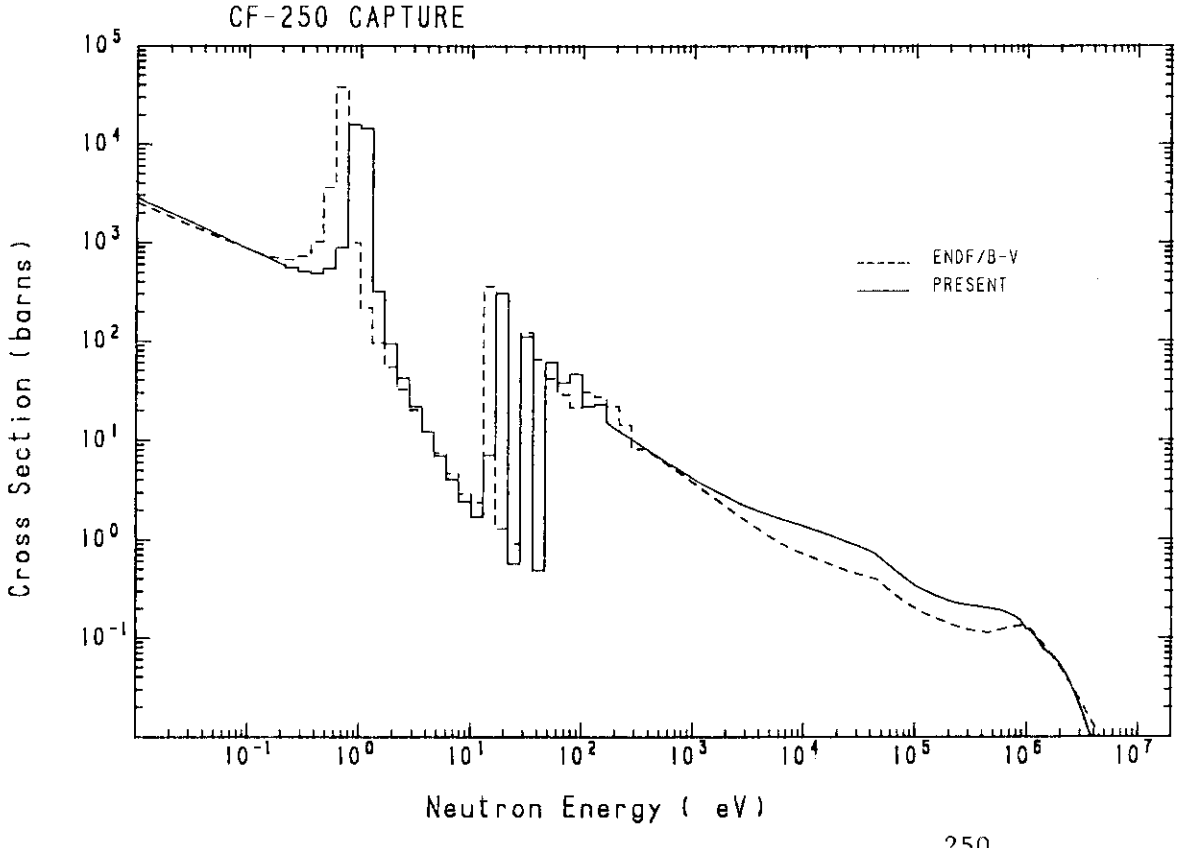

Fig. 8 The radiative capture cross section of ^{250}Cf

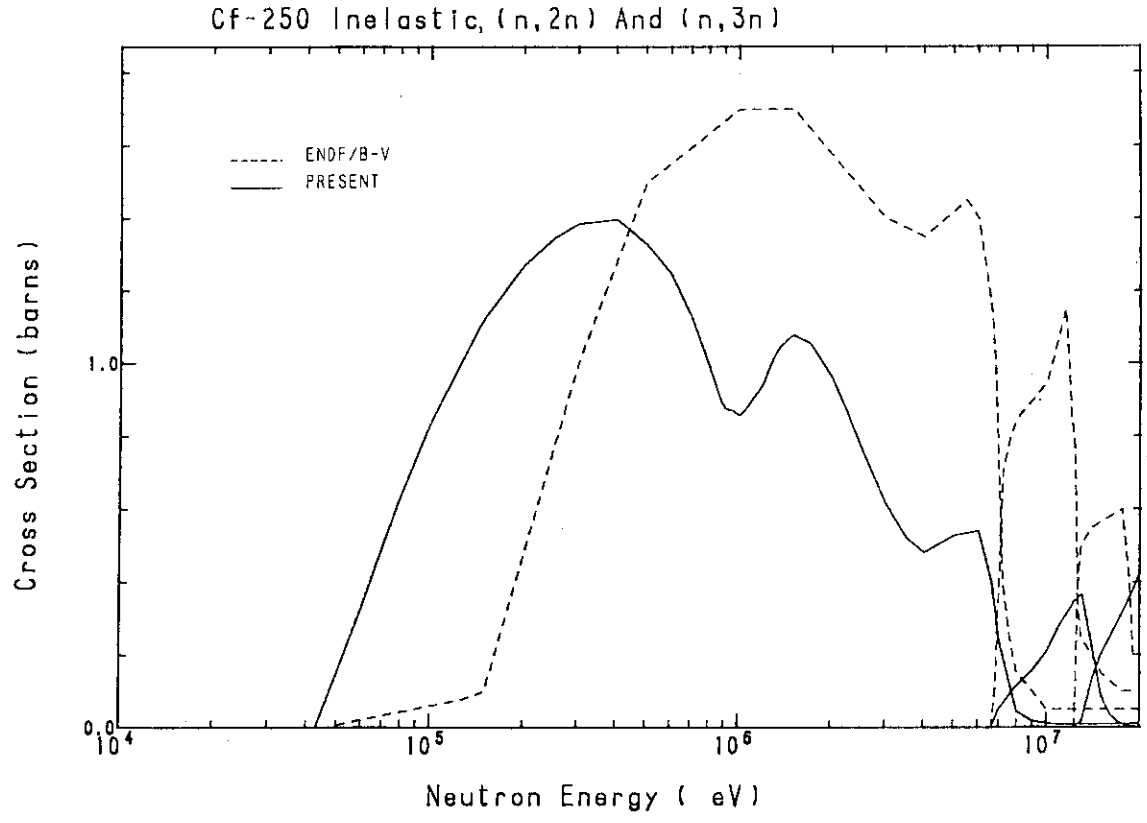

Fig. 9 The inelastic scattering, (n,2n) and (n,3n) reaction cross sections of ^{250}Cf

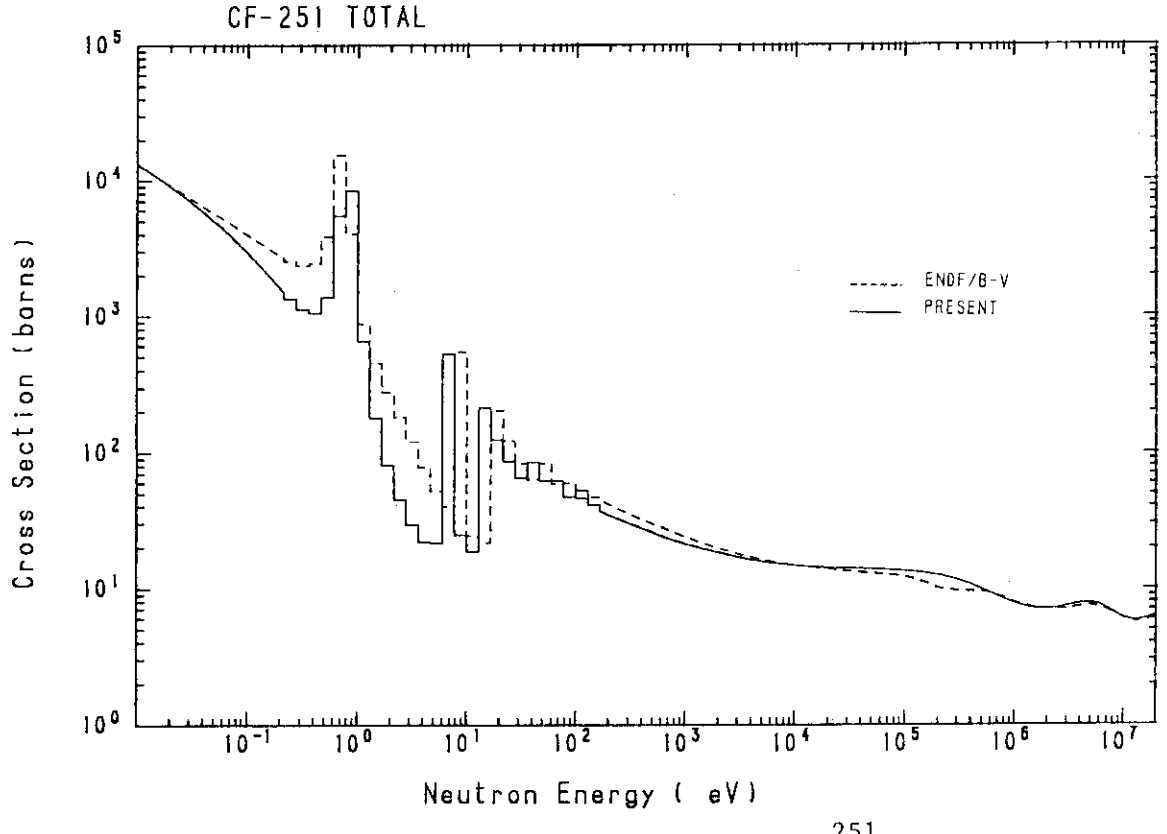

Fig. 10 The total cross section of ^{251}Cf

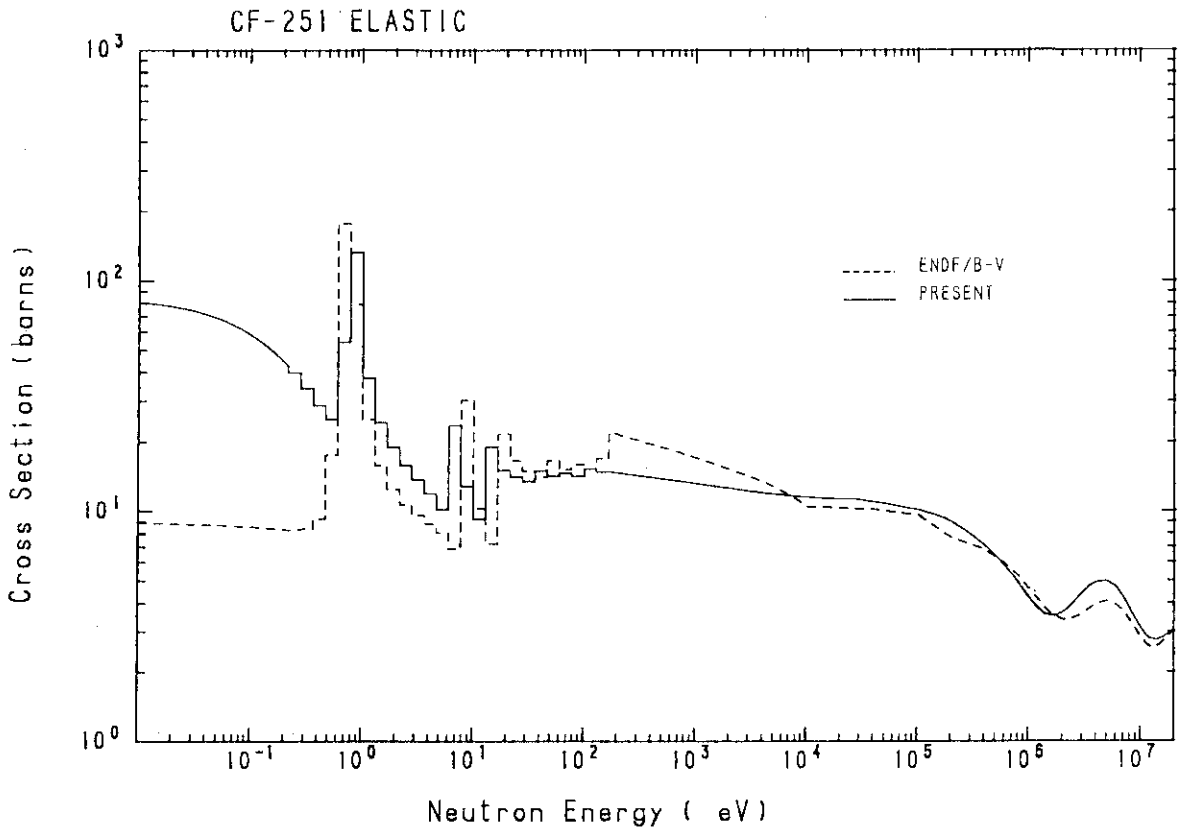

Fig. 11 The elastic scattering cross section of ^{251}Cf

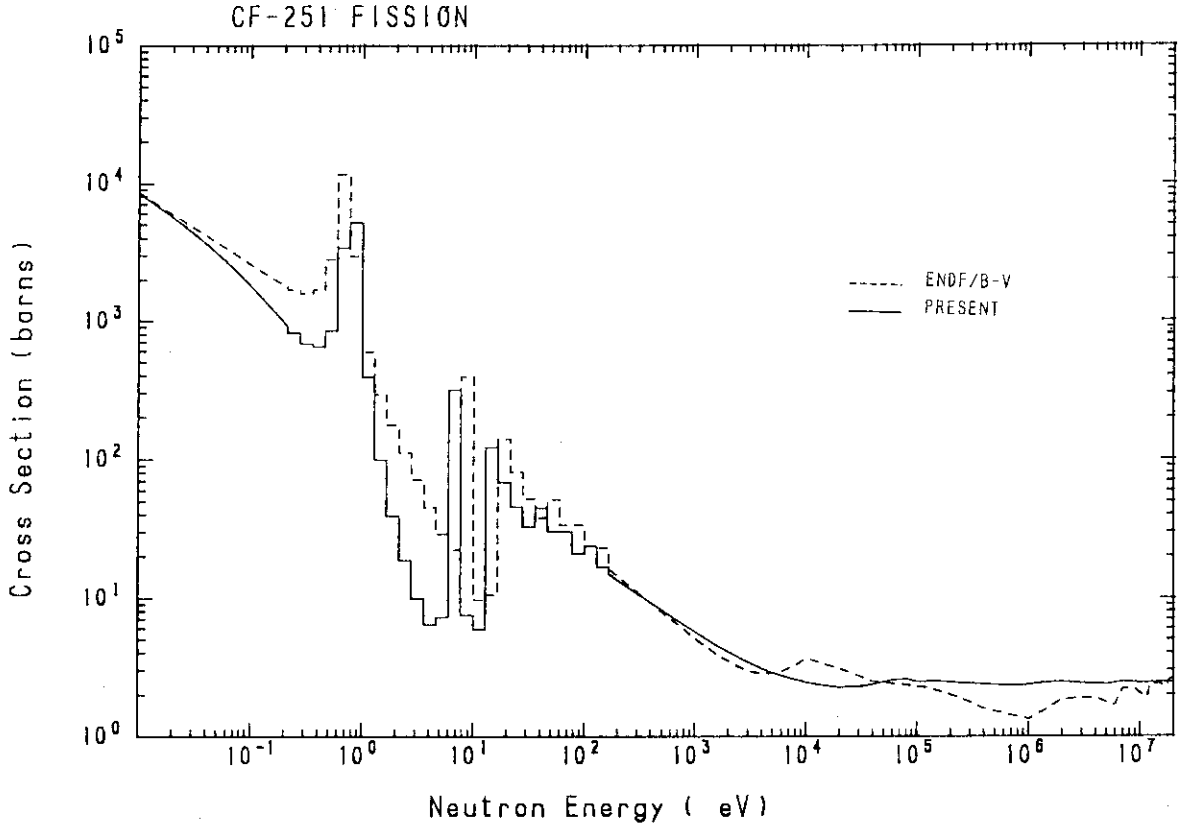

Fig. 12 The fission cross section of ^{251}Cf

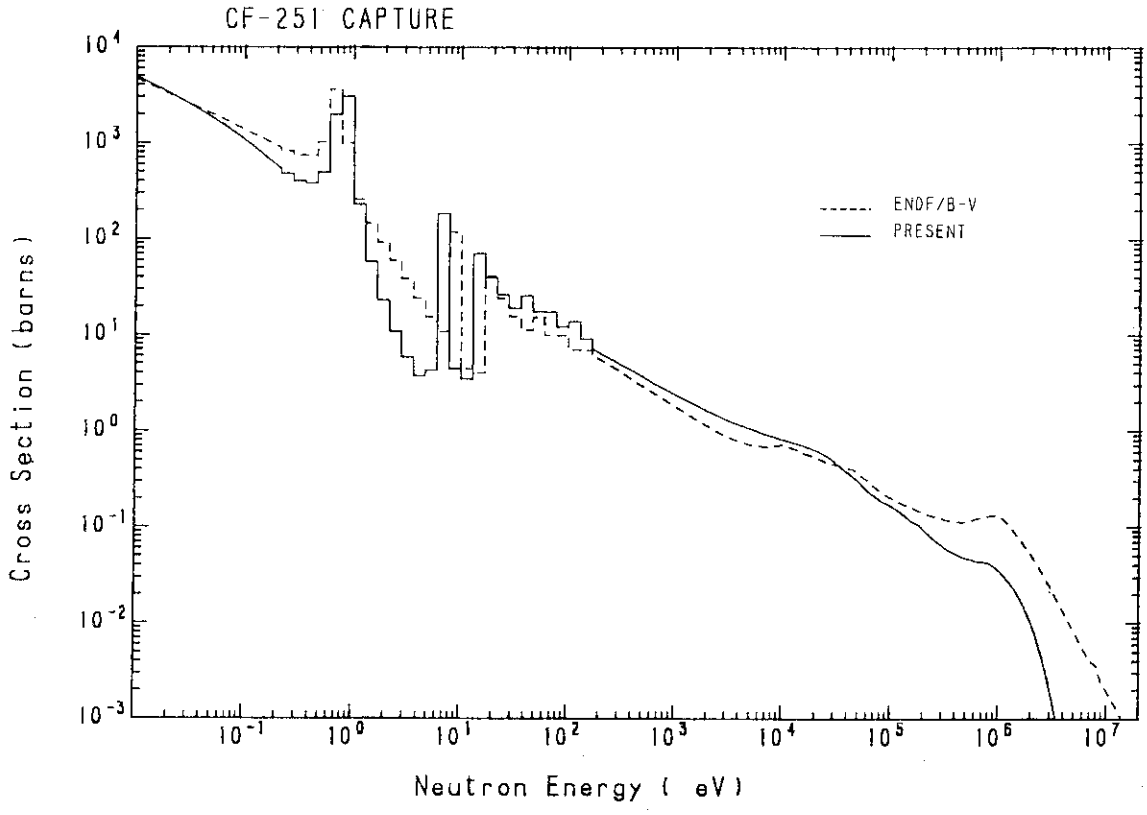

Fig. 13 The radiative capture cross section of ^{251}Cf

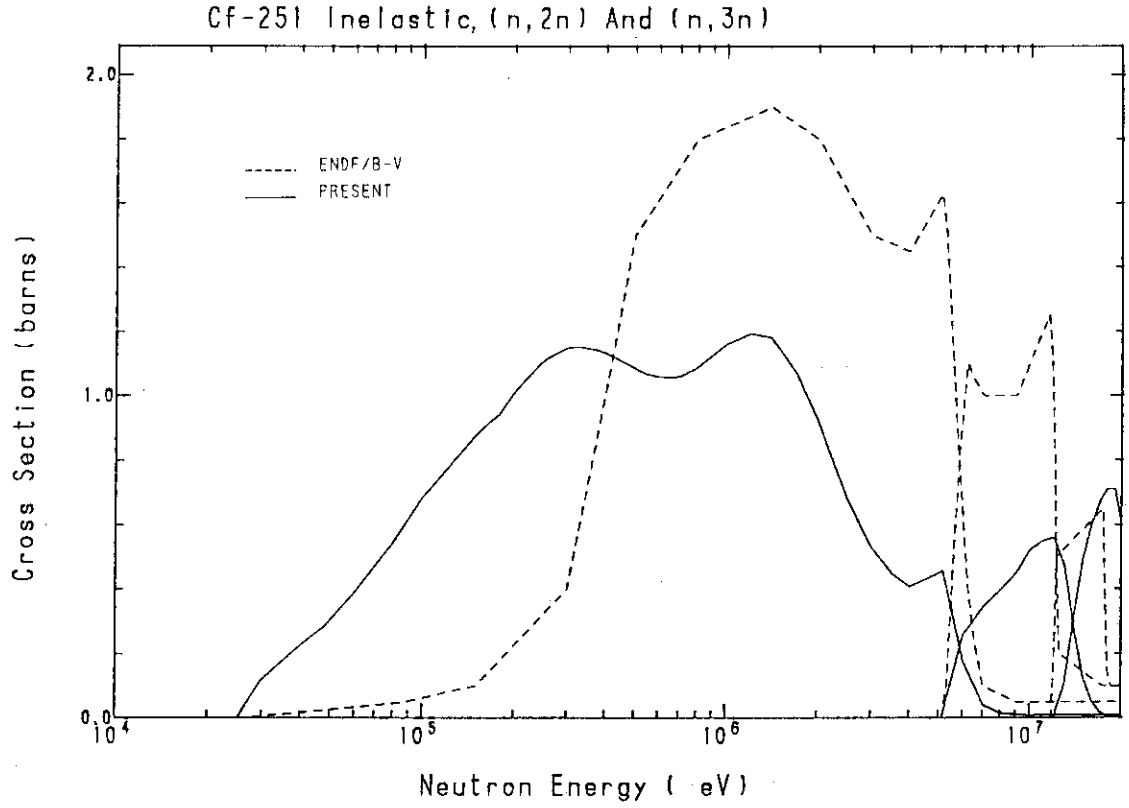

Fig. 14 The inelastic scattering, (n,2n) and (n,3n) reaction cross sections of ^{251}Cf

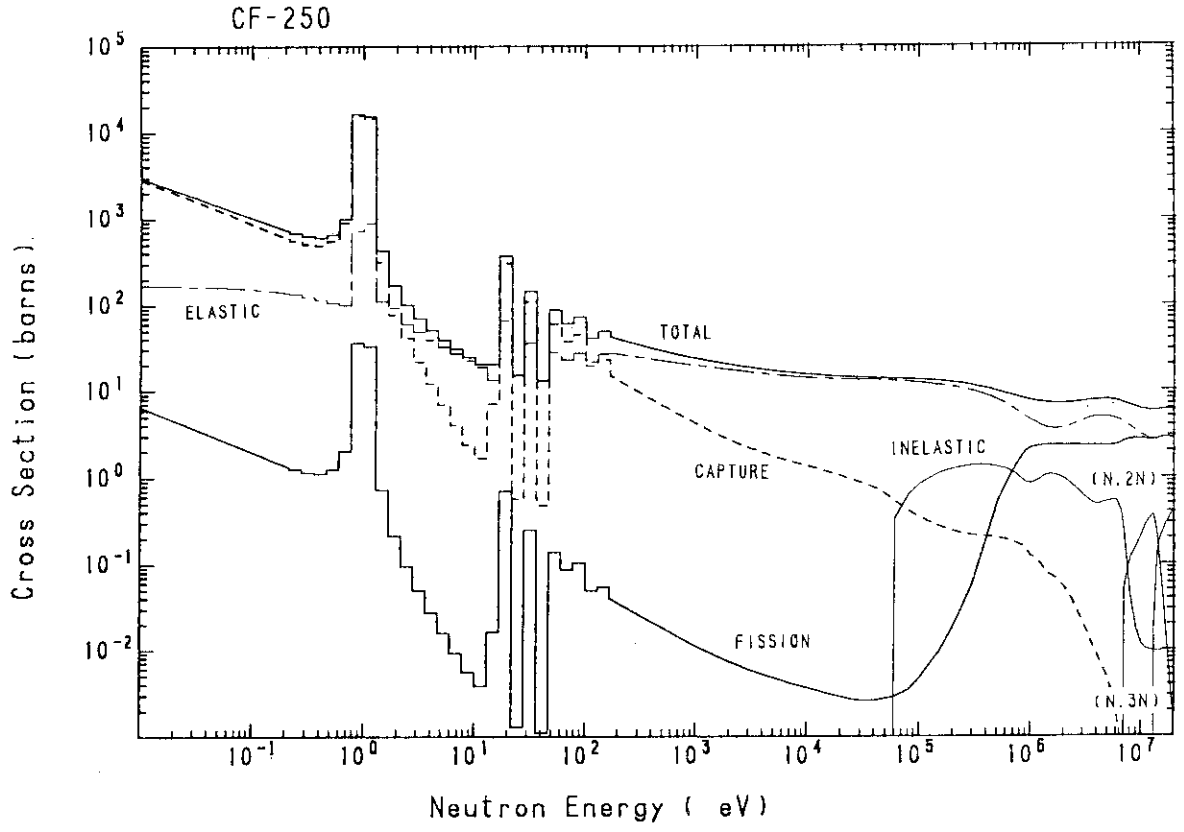

Fig. 15 The cross sections of ^{250}Cf

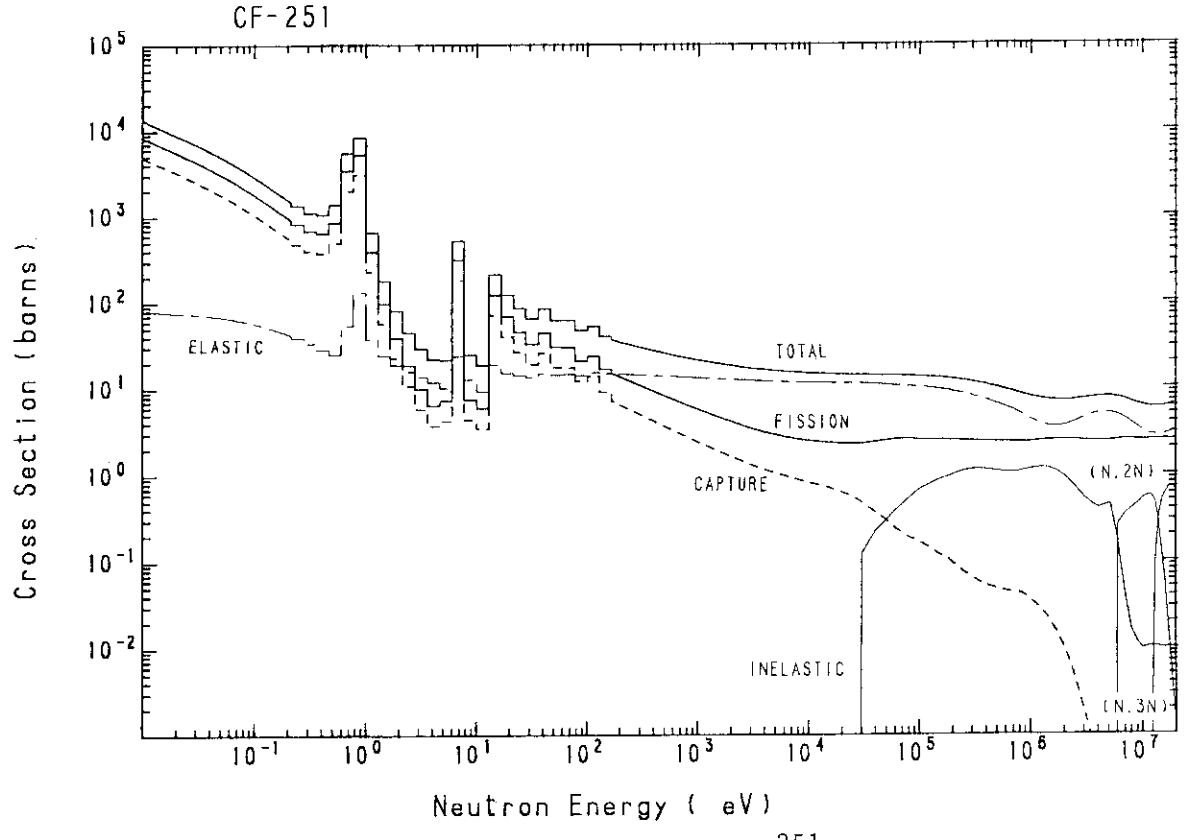

Fig. 16 The cross sections of ^{251}Cf